Combination of Backstepping and Reduced Indirect FCS-MPC for Modular Multilevel Converters

Saad Hamayoon[1], Morten Hovd[1] and Jon Are Suul[2]
[1]*Department of Engineering Cybernetics, Norwegian University of Science and Technology, Trondheim, Norway*
[2]*SINTEF Energy Research, Trondheim, Norway*
email:saad.hamayoon@ntnu.no

***Abstract*—In this paper, backstepping is applied as a first step of modulation control in the abc reference frame for modular multilevel converters (MMCs). In the second step, reduced indirect FCS-MPC is applied where the number of inserted modules are allowed to change by maximum one from the rounded result of the continuous outcome from backstepping. The backstepping method uses the ac-side current, differential current and summation of capacitor voltages in one arm as the state variables to form the Lyapunov functions. An established bilinear model of MMCs is used in the proposed design. The proposed approach offers similar dynamic performance as the full indirect FCS-MPC, at a much lower computational burden. The performance of the proposed method is validated by simulation.**

***Index Terms*—backstepping, differential current, model predictive control, modular multilevel converter (MMC), capacitor voltage balancing, Lyapunov stability**

I. Introduction

Modular multilevel converters (MMCs) are becoming the dominant technology for high voltage direct current (HVDC) transmission systems [1]. This is due to their excellent features in terms of scalability and applicability to high voltage systems resulting from their modular nature that enables them to attain any number of voltage levels. The higher number of voltage levels also allows for reduced filtering requirements. Moreover, MMCs offer redundancy *i.e.* faulty submodules (SMs) can be easily bypassed.

The control of MMCs is complex due to the non-linearities and the multi-input multi-output (MIMO) nature of the resulting system. The control strategy for MMCs has to meet multiple objectives *i.e.* control of the output current, the circulating currents and balancing of SM capacitor voltages. In the literature, many control techniques have been proposed for MMCs [2]–[4]. These methods include linear as well as non-linear controllers. However, with increasing research activities on non-linear methods, specific challenges of application to MMCs are now being considered, for instance model predictive control [4], sliding mode control [6], feedback linearization [7] and backstepping [8]–[10].

Model predictive control (MPC) is an effective technique to address the MIMO nature and non-linearities of the system. In power converters, usually finite control set model predictive control (FCS-MPC) is used. However, for MMCs the computational complexity of FCS-MPC is very high due to the high sampling rates and large number of SMs per arm. Therefore, significant efforts are being done to reduce the computational complexity of MPC [11]–[15]. However, these approaches either suffer from slow dynamic performance or or impose very high computational requirements when the number of SMs per arm are high. The sliding mode control suffers from chattering problem while feedback linearization often cancels out useful non-linearities [16]. Among the mentioned techniques, only backstepping does not suffer from aforementioned problems. However, the backstepping control used in [8] studies only the inverter operation of MMC. Moreover, a separate modulation stage is required. The backstepping controller in [9], [10] works in the $\alpha\beta$ reference frame and the dq reference frame respectively which does not directly allow for controlling each phase independently.

In this work, backstepping is applied as a first step of modulation control for modular multilevel converters (MMCs). The solution obtained from backstepping is continuous, however, the voltage level can only be discrete for MMC. Therefore, the solution is rounded off to the nearest integer. In the next step, reduced indirect FCS-MPC is applied where the number of inserted SMs are allowed to change by a maximum of one from the rounded result obtained by backstepping. Each option as a result of this change is evaluated by a predefined cost function and the option which gives the minimal cost is then selected for the generation of MMC arm voltage outputs. The proposed work offers high dynamic performance at a low computational burden by combining the benefits of backstepping and reduced indirect FCS-MPC.

The rest of the paper is organized as follows. The modeling and operation of the MMC is presented in Section II. The proposed method is discussed in Section III. Furthermore, for performance validation of the proposed method, simulation results are presented in Section IV.

II. Model of the MMC

The model applied in this paper is developed from [18]. The configuration of the three-phase MMC system used in this paper is shown in Fig. 1. The MMC consists of two identical arms *i.e.* an upper arm and a lower arm in each phase which are connected to the positive and negative dc terminal, respectively. The subscripts u and l are used for upper and lower arm respectively. Each arm consist of N half-bridge submodules (SM), an inductor and a resistor. The arm resistance models the losses of the MMC and the arm

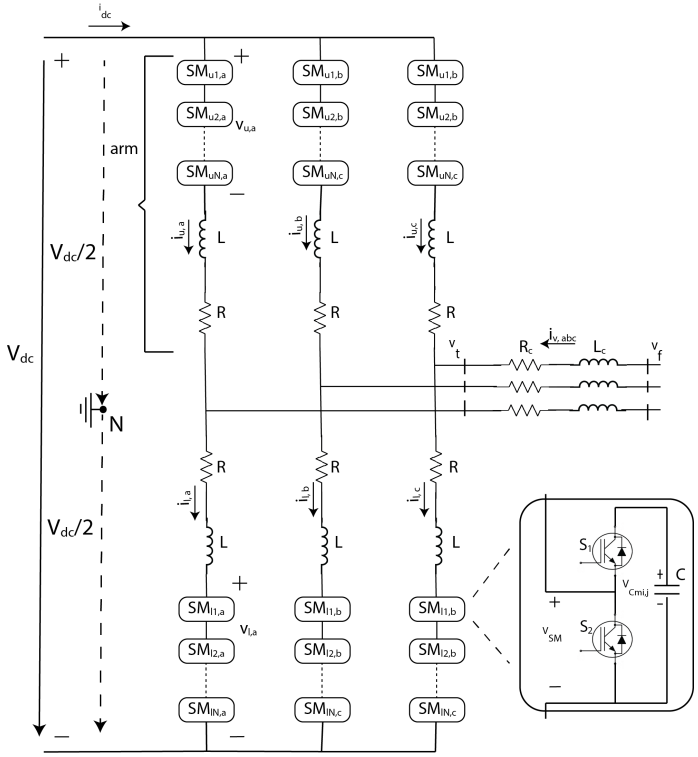

Fig. 1. Circuit Diagram of MMC

inductor is used for limiting the harmonics and fault currents. The switching states of S_1 and S_2 determine the voltage level for each SM. The voltage level can be *i.e.* 0 or $v_{\mathrm{Cm_{i,j}}}$ where the index $m = u, l$ identifies the upper or lower arm, $i = 1, 2, \ldots, N$ identifies the individual sub-module within the arm, and $j = a, b, c$ identifies the phase.

The mathematical model of the MMC shown in Fig 1, can be expressed as according to Kirchoff's voltage law:

$$\frac{V_{dc}}{2} - v_{u,j} - Ri_{u,j} - L\frac{di_{v,j}}{dt} + R_c i_{v,j} + L_c \frac{di_{v,j}}{dt} - v_f = 0 \quad (1)$$

$$\frac{V_{dc}}{2} - v_{l,j} - Ri_{l,j} - L\frac{di_{l,j}}{dt} - R_c i_{v,j} - L_c \frac{di_{v,j}}{dt} + v_f = 0 \quad (2)$$

where $v_{u,j}$ and $v_{l,j}$ represent the upper and lower arm voltages of phase j, $i_{u,j}$ and $i_{l,j}$ represent the upper and lower arm currents of phase j, $i_{v,j}$ is the ac-side current, V_{dc} is the dc-side voltage, v_f is the grid side voltage, R is the arm resistance, L is the arm inductance, R_c and L_C are the equivalent grid side resistance and inductance, respectively.

The ac-side current, arm currents and differential currents are given by:

$$i_{v,j} = i_{l,j} - i_{u,j} \quad (3)$$

$$i_{u,j} = -\frac{i_{v,j}}{2} + \frac{i_{diffj}}{2} \quad (4)$$

$$i_{l,j} = \frac{i_{v,j}}{2} + \frac{i_{diffj}}{2} \quad (5)$$

where i_{diffj} is the differential current which flows through each of the three phases of the MMC.

By subtracting (1) and (2) and using (3) the dynamic equation for ac-side current is obtained as:

$$\frac{di_{v,j}}{dt} = \frac{-(R+2R_c)}{L+2L_c} i_{v,j} + \frac{v_{u,j} - v_{l,j}}{L+2L_c} + \frac{2v_{f,j}}{L+2L_c} \quad (6)$$

Similarly, by adding (1) and (2) and using (4) and (5), the dynamic equation for the differential current is obtained as:

$$\frac{di_{diff,j}}{dt} = \frac{-R}{L} i_{diff,j} - \frac{1}{2L}(v_{u,j} + v_{l,j}) + \frac{1}{2L} V_{dc} \quad (7)$$

The arm voltages $v_{u,j}$ and $v_{l,j}$ depend on the number of SMs inserted in that arm. Assuming that SM capacitor voltages are well balanced at their reference values, the arm voltages can be expressed as:

$$v_{u,j} \approx \frac{n_{u,j}}{N} v^{\Sigma}_{u,j} \quad (8)$$

$$v_{l,j} \approx \frac{n_{l,j}}{N} v^{\Sigma}_{l,j} \quad (9)$$

where $n_{u,j}$ and $n_{l,j}$ are the insertion indices *i.e.* number of SMs to be inserted in upper and lower arm respectively and $v^{\Sigma}_{u,j}$ and $v^{\Sigma}_{l,j}$ are the summation of all capacitor voltages in the upper and lower arm respectively.

The dynamics of the total arm capacitor voltages can be expressed as:

$$\frac{dv^{\Sigma}_{m,j}}{dt} = \frac{i_{m,j}}{C^e_{m,j}} = \frac{n_{m,j} i_{m,j}}{C} \quad (10)$$

where $C^e_{m,j}$ is the equivalent arm capacitance of inserted SMs in arm m. Now equations (4) and (5) can be substituted into (10) to give the following dynamic equations for total arm capacitor voltages of both arms:

$$\frac{dv^{\Sigma}_{u,j}}{dt} = -\frac{n_{u,j} i_{v,j}}{2C} + \frac{n_{u,j} i_{diff,j}}{C} \quad (11a)$$

$$\frac{dv^{\Sigma}_{l,j}}{dt} = \frac{n_{l,j} i_{v,j}}{2C} + \frac{n_{l,j} i_{diff,j}}{C} \quad (11b)$$

Using the definition of $v_{u,j}$ and $v_{l,j}$ from (8) and (9) into (6) and (7) the dynamic equations for ac-side current and differential current are modified as:

$$\frac{di_{v,j}}{dt} = \frac{-(R+2R_c)}{L+2L_c} i_{v,j} + \frac{n_{u,j} v^{\Sigma}_{u,j} - n_{l,j} v^{\Sigma}_{l,j}}{N(L+2L_c)} + \frac{2v_{f,j}}{L+2L_c} \quad (12a)$$

$$\frac{di_{diff,j}}{dt} = \frac{-R}{L} i_{diff,j} - \frac{(n_{u,j} v^{\Sigma}_{u,j} + n_{l,j} v^{\Sigma}_{l,j})}{2NL} + \frac{V_{dc}}{2L} \quad (12b)$$

Using (11) and (12) the state space equation for one phase/leg of the three phase MMC is shown by (13)

$$\dot{x}(t) = Ax(t) + \sum_{i=1}^{2} (B_{ix} u_i) + d(t) \quad (13)$$

where $x = [i_{v,j}, i_{diff,j}, v^{\Sigma}_{u,j}, v^{\Sigma}_{l,j}]^T$ is the state vector, $u = [u_1 u_2]^T = [n_{u,j} n_{l,j}]^T$ is the input vector, $d(t)$ is the disturbance and

$$A = \begin{bmatrix} -\frac{(R+2R_c)}{L+2L_c} & 0 & 0 & 0 \\ 0 & -\frac{R}{L} & 0 & 0 \\ 0 & 0 & 0 & 0 \\ 0 & 0 & 0 & 0 \end{bmatrix}$$

$$B_{ix} = \begin{bmatrix} B_1 x(t) & B_2 x(t) \end{bmatrix}$$

$$B_1 = \begin{bmatrix} 0 & 0 & \frac{1}{(L+2L_c)N} & 0 \\ 0 & 0 & \frac{-1}{2NL} & 0 \\ \frac{-1}{2C} & \frac{1}{C} & 0 & 0 \\ 0 & 0 & 0 & 0 \end{bmatrix}$$

$$B_2 = \begin{bmatrix} 0 & 0 & 0 & \frac{-1}{(L+2L_c)N} \\ 0 & 0 & 0 & \frac{-1}{2NL} \\ 0 & 0 & 0 & 0 \\ \frac{1}{2C} & \frac{1}{C} & 0 & 0 \end{bmatrix}$$

$$d(t) = \begin{bmatrix} \frac{2v_{f,j}(t)}{(L+2L_c)} \\ \frac{V_{dc}(t)}{2L} \\ 0 \\ 0 \end{bmatrix}$$

Equation (13) shows that the MMC is a bilinear system with multiple inputs and outputs.

III. Proposed Control Method for the MMC

A. Backstepping Design

In this work, the ac-side current $i_{v,j}$, differential current $i_{diff,j}$, summation of upper and lower arm capacitor voltages $v_{u,j}^{\Sigma}, v_{l,j}^{\Sigma}$ are used as the state variables. Then based on these state variables, the error variables for backstepping are given as follows:

$$e_1 = i_{diffref,j} - i_{diff,j} \tag{14}$$

$$e_2 = V_{dc,ref} - v_{u,j}^{\Sigma} \tag{15}$$

$$e_3 = V_{dc,ref} - v_{l,j}^{\Sigma} \tag{16}$$

$$e_4 = i_{vref,j} - i_{v,j} \tag{17}$$

Based on above errors, the following four Lyapunov functions (LF) were formed for backstepping design:

$$V_1 = \frac{1}{2}e_1^2 \tag{18}$$

$$V_2 = V_1 + \frac{1}{2}e_2^2 \tag{19}$$

$$V_3 = V_2 + \frac{1}{2}e_3^2 \tag{20}$$

$$V_4 = V_3 + \frac{1}{2}e_4^2 \tag{21}$$

Before proceeding with backstepping design, it is noted that the reference for summation voltages are constant. Moreover, the reference for differential current is also constant for a fixed power. Therefore, their derivatives would be zero in steady state. Only the reference of ac-side current would be varying and its derivative would exist.

It can be observed that the LFs are positive in (18-21). Based on Lyapunov theory, the time-based derivative of these functions must be negative. Using (11) and (12) and taking derivatives of the LFs the following expressions are obtained:

$$\dot{V}_1 = e_1(\frac{R}{L}i_{diff,j} + \frac{(n_{u,j}v_{u,j}^{\Sigma} + n_{l,j}v_{l,j}^{\Sigma})}{2NL} - \frac{V_{dc}}{2L}) \tag{22}$$

$$\dot{V}_2 = e_2(\frac{n_{u,j}i_{v,j}}{2C} - \frac{n_{u,j}i_{diff,j}}{C}) + \dot{V}_1 \tag{23}$$

$$\dot{V}_3 = e_3(-\frac{n_{l,j}i_{v,j}}{2C} - \frac{n_{l,j}i_{diff,j}}{C}) + \dot{V}_2 \tag{24}$$

$$\dot{V}_4 = e_4(\dot{i}_{vref,j} + \frac{(R+2R_c)}{L+2L_c}i_{v,j} - \frac{n_{u,j}v_{u,j}^{\Sigma} - n_{l,j}v_{l,j}^{\Sigma}}{N(L+2L_c)} - \frac{2v_{f,j}}{L+2L_c}) + \dot{V}_3 \tag{25}$$

The LF in (25) includes the effect of all the LFs. Therefore, ensuring negativity of (25) would guarantee that the system is indeed stable. So, the designed controller should ensure that $\dot{V}_4$ is negative.

It is noted that there are two control inputs for each phase of the MMC *i.e.* $n_{u,j}$ and $n_{l,j}$ for each arm. However, there is only one equation *i.e.* (25), therefore a relation between these two controllers is required to proceed further with the design. In [17] different control choices for these controllers are shown. In this work, the following relation between the two controllers is utilized.

$$n_{u,j} = N - n_{l,j} \tag{26}$$

It is noted here, that (26) may not result in optimal performance of the MMC. This is because (26) is the ideal case for continuous approximation of insertion indices and does not consider the need for controlling the differential current. Therefore, an idea from indirect FCS-MPC is presented later to deal with this. By using (26) in (25) and after some simplification the following expression is achieved.

$$\dot{V}_4 = n_{u,j}H + \frac{e_1 v_{l,j}^{\Sigma}}{2L} + e_3 N(\frac{-i_{v,j}}{2C} - \frac{i_{diff,j}}{C}) + \frac{e_4 v_{l,j}^{\Sigma}}{L+2L_c} + e_1(\frac{R}{L}i_{diff,j} - \frac{V_{dc}}{2L}) + e_4(\dot{i}_{vref,j} + \frac{(R+2R_c)}{L+2L_c}i_{v,j} - \frac{2v_{f,j}}{L+2L_c}) \tag{27}$$

where

$$H = \frac{e_1 v_{u,j}^{\Sigma}}{2NL} + e_2(\frac{i_{v,j}}{2C} - \frac{i_{diff,j}}{C}) - \frac{e_4 v_{u,j}^{\Sigma}}{N(L+2L_c)} - \frac{e_1 v_{l,j}^{\Sigma}}{2NL} - e_3(\frac{-i_{v,j}}{2C} - \frac{i_{diff,j}}{C}) - \frac{e_4 v_{l,j}^{\Sigma}}{N(L+2L_c)} \tag{28}$$

So, now the control law $n_{u,j}$ that will guarantee system stability and negative time derivative of the LF is selected as:

$$n_{u,j} = \frac{1}{H}(-\frac{e_1 v_{l,j}^{\Sigma}}{2L} - e_3 N(\frac{-i_{v,j}}{2C} - \frac{i_{diff,j}}{C}) - \frac{e_4 v_{l,j}^{\Sigma}}{L+2L_c} - e_1(\frac{R}{L} i_{diff,j} - \frac{V_{dc}}{2L}) - e_4(\dot{i}_{vref,j} + \frac{(R+2R_c)}{L+2L_c} i_{v,j} - \frac{2v_{f,j}}{L+2L_c}) - c_1 e_1^2 - c_2 e_2^2 - c_3 e_3^2 - c_4 e_4^2) \quad (29)$$

The above control law will give the following expression:

$$\dot{V}_4 = -c_1 e_1^2 - c_2 e_2^2 - c_3 e_3^2 - c_4 e_4^2 \quad (30)$$

Therefore, to ensure that (30) is negative all the coefficients c_i must be positive. These coefficients can also impact the control design. In this work, no specific criteria is used to determine them. However, it was noted that by increasing the values of these coefficients (up to a certain limit) the errors were reduced. In this paper, all coefficients are kept equal to a value of 250 as increasing beyond this value resulted in increase in the errors. It is also noted that if the expression H results in a very small number then there is a possibility of using excessively large control inputs. On analyzing H, it is noted that only e_4 terms will have significant contribution. Therefore, whenever the absolute value of e_4 is small, its absolute value is increased by 1 or -1 depending on the sign of e_4, to avoid excessively large input values. It is also worth mentioning here that the above design can be simplified further by only considering e_1 and e_4 and setting e_2, e_3 equal to zero. This can be seen from (11) where the summation voltages are depending on the other two state variables and control input. Therefore, if the other two state variables are well regulated then summation voltages should automatically regulate themselves. The same is done in this paper. This simplifies (29) significantly.

The controllers returned by above design would be continuous. However, the voltage levels of the MMC can only be discrete. Therefore, the above solutions are rounded off to the nearest integer. Then (26) can be utilized to find the other controller. However, as previously mentioned, (26) will not necessarily result in optimal performance. Thus, the idea from indirect FCS-MPC is utilized.

B. FCS-MPC

In FCS-MPC, all possible switching combinations of the power converter are used to evaluate a predefined cost function. The switching combination that minimizes this cost function is then applied to the power converter over the next sampling interval [5]. In this work, the idea from indirect FCS-MPC is utilized where the optimized voltage level is used to minimize the cost function instead of optimum switching combination [5]. However, instead of considering all the possible voltage levels only the voltage levels in the vicinity of inputs returned by backstepping controllers are considered. This vicinity is limited to a maximum change of 1 as in [5]. This results in a total of 9 options in each time step. The

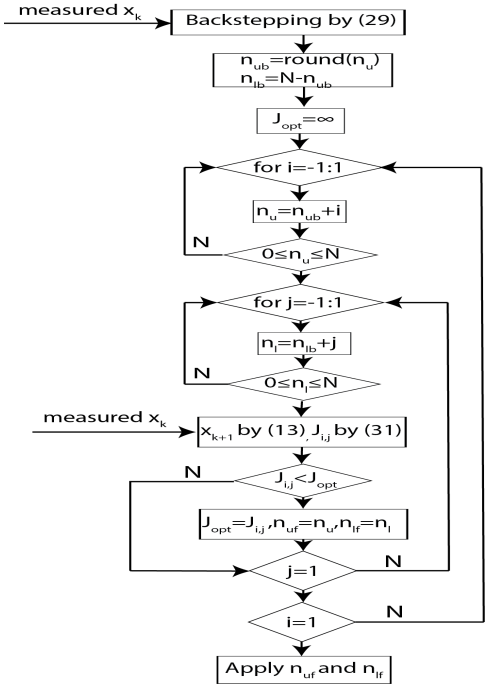

Fig. 2. Block diagram for Proposed Method

TABLE I
COMPARISON OF DIFFERENT FCS-MPC STRATEGIES

Methodology (N=20)	**Comparison**		
	No. of Control Options p=3	**No. of FLOPS p=1**	**Elapsed Time (ms) p=1**
Full Indirect FCS-MPC	85,766,121	55,338	6.7
Reduced Indirect FCS-MPC	729	1242	3.4
Modified Reduced Indirect FCS-MPC	2025	3450	3.8
Proposed	729	1413	3.5

comparison of different approaches for a prediction horizon (indicated by p) for an MMC with 20 SMs per arm is shown in Table-I. It is noted that the elapsed time was calculated using MATLAB R2019b on Intel® Core i7, 3.20 GHz, with 16 GB RAM. Therefore, the computation times would be lower for all cases with efficient implementation on a dedicated real time platform (without much of the overhead of the operating system on a general purpose computer). It can be seen that the proposed approach has much lower computational burden as compared to full indirect FCS-MPC and similar computational complexity as reduced indirect FCS-MPC. However, the proposed method has similar dynamic performance as full indirect FCS-MPC which will be demonstrated by simulation results. It is further noted that the proposed approach is relatively insensitive to the number of SMs per arm. For MMCs with a large number of SMs, reduced indirect FCS-MPC and it's variants would require considering more levels in the first step for better dynamic response [18], leading to corresponding increase in calculation requirements.

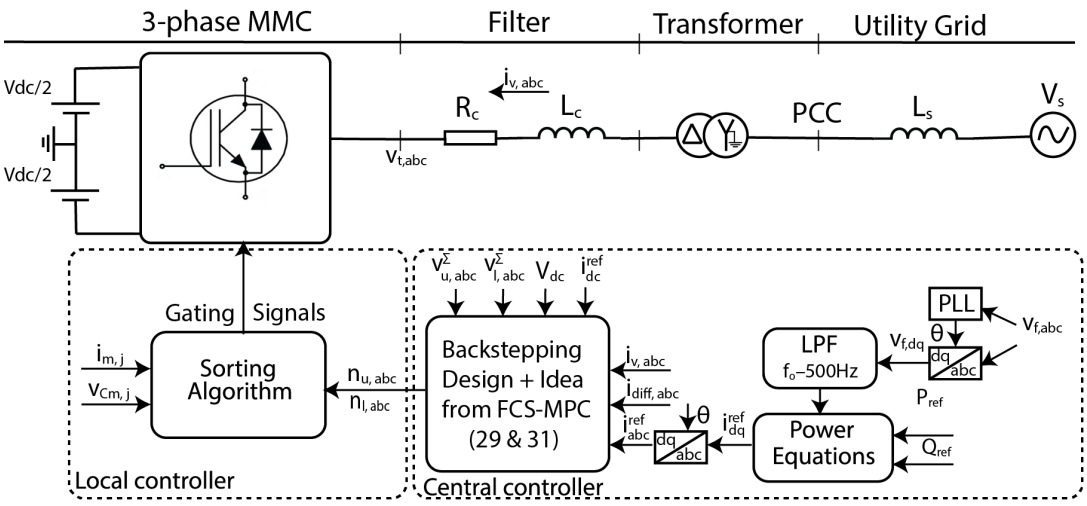

Fig. 3. Control Block Diagram of MMC

The cost function utilized for this purpose is given as follows:

$$J_j = \lambda_1 |i_{v,j,ref} - i_{v,j}| + \lambda_2 |i_{diff,ref} - i_{diff,j}| \tag{31}$$

where λ_1 = 1 and λ_2 = 0.5.

The flowchart for the proposed approach is shown in fig. 2 where (13) is discretized using forward Euler approximation.

The reference for differential current, summation voltages and ac-side current are as in [18] and the conventional sorting algorithm is used for SM capacitor voltage balancing task as in [18]. However, for the sake of completeness the references selection is repeated here. The power equations in the dq frame are used to obtain the reference value for the ac-side current as follows:

$$i_d = \frac{2}{3}\frac{Pv_d + Qv_q}{v_d^2 + v_q^2} \tag{32a}$$

$$i_q = \frac{2}{3}\frac{Pv_q - Qv_d}{v_d^2 + v_q^2} \tag{32b}$$

Then by dq to abc transformation, the abc frame reference current can be obtained. The reference for the differential current is given as:

$$I_{dc,ref} = -\frac{P}{V_{dc,ref}}, I_{diff,ref} = -\frac{I_{dc,ref}}{3} \tag{33}$$

However, it is noted here that differential current reference needs to be adjusted to regulate the summation voltages [1].

IV. Simulation Results

The block diagram for calculation of insertion indices through the proposed methodology is shown in Fig. 3. The scenario used for simulation is such that, at t=0s the reference values of active and reactive power are set to 25 MW and 0 MVar , respectively and at t = 0.12s a real power reversal command is applied by changing active power set point to -25 MW. The parameters used for simulation are summarized in Table-II.

TABLE II
Simulation Parameters

Parameter	Value
MMC nominal power (base power)	50 MVA
AC system nominal voltage (base voltage)	138 kV
Short circuit ratio at PCC	5
AC source inductance (Ls)	150 mH
Nominal frequency	60 Hz
Arm inductance (L)	7 mH
Arm resistance (R)	1Ω
Submodule capacitance (C)	14000μF
Transformer voltage rating (T)	138 kV / 30 kV
Transformer power rating	55 MVA
Transformer inductance	0.05 pu
Transformer resistance	0.01 pu
Grid side converter inductance (Lc)	5 mH
Grid side converter resistance (Rc)	0.03Ω
DC side reference voltage	60 kV
Number of SMs per arm (N)	20
Sampling time (Ts)	100μs

Figure 4 shows the performance of all the state variables being controlled by the proposed method under active power reversal command. In Fig. 4(a) the changes in the active and reactive power are shown. In Fig. 4(b) the phase-a current is shown. It can be observed that the dynamic response is very good. The differential current performance of phase a is shown in Fig. 4(c) which shows that it tracks it's reference both in steady-state as well as in transient state. The summation of capacitor voltages in the upper arm of phase a are depicted in Fig. 4(d). It can be seen that the average value of summation voltages is around their reference.

In fig. 5, the d-axis current component of the ac-side current is shown where dynamic response of the proposed method is compared with three other strategies *i.e.*, reduced indirect FCS-

MPC [5], full indirect FCS-MPC [5] and modified reduced indirect FCS-MPC [18]. This validates the superior dynamic performance of proposed method in comparison to the reduced indirect FCS-MPC in [6] and shows nearly the same dynamic performance to full and modified indirect FCS-MPC at a much lower computational complexity.

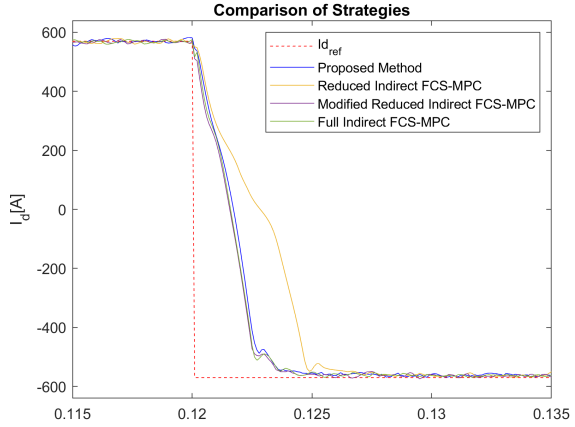

Fig. 5. Comparison of Results for d-axis component of ac-side current

V. Conclusion

In this work, a method based on combination of backstepping and reduced indirect FCS-MPC is proposed for MMC. In the proposed strategy, the number of inserted SMs are allowed a maximum change of one from the rounded off result obtained from backstepping. A single cost function per phase was designed to select the optimal insertion index of each arm in order to minimize the error in ac-side current tracking and to minimize the ac-component of differential current. The conventional sorting algorithm was used to perform the voltage balancing task. Simulations demonstrate that the proposed method gives a very good steady-state and dynamic performance. Moreover, as compared to conventional FCS-MPC techniques the computational burden of proposed method is significantly reduced and is relatively independent of nunber of SMs/arm, while offering comparable dynamic response. This allows the proposed method to be used with an extended prediction horizon.

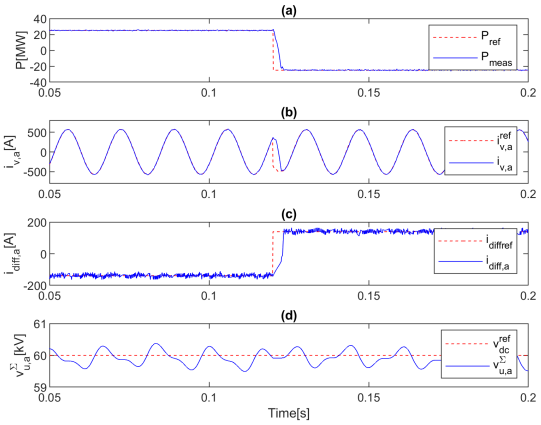

Fig. 4. Backstepping: (a) real and reactive power, (b) phase-a current, (c) phase-a differential current, (d) summation of the capacitor voltages in the upper arm of phase a

References

[1] K. Sharifabadi, L. Harnefors, H.-P. Nee, S. Norrga, and R. Teodorescu, *Design, Control and Application of Modular Multilevel Converters for HVDC Transmission Systems.* United States: Wiley-IEEE press, 2016.

[2] A. Dekka, B. Wu, R. L. Fuentes, M. Perez and N. R. Zargari, "Evolution of Topologies, Modeling, Control Schemes, and Applications of Modular Multilevel Converters," *IEEE Journal of Emerging and Selected Topics in Power Electronics,* vol. 5, no. 4, pp. 1631-1656, Dec 2017

[3] A. Antonio-Ferreira, C. Collados-Rodriguez and O. Gomis-Bellmunt, "Modulation techniques applied to medium voltage modular multilevel converters for renewable energy integration: A review", *Electric Power Systems Research,* vol. 155, no. 7, pp. 21-39, Feb 2018

[4] S. Debnath, J. Qin, B. Bahrani, M. Saeedifard and P. Barbosa, "Operation, Control, and Applications of the Modular Multilevel Converter: A Review," *IEEE Transactions on Power Electronics*, vol. 30, no. 1, pp. 37-53, Jan. 2015

[5] M. Vatani, B. Bahrani, M. Saeedifard and M. Hovd, "Indirect Finite Control Set Model Predictive Control of Modular Multilevel Converters," *IEEE Transactions on Smart Grid,* vol. 6, no. 3, pp. 1520-1529, May 2015

[6] Q. Yang, M. Saeedifard and M. A. Perez, "Sliding Mode Control of the Modular Multilevel Converter," *IEEE Transactions on Industrial Electronics*, vol. 66, no. 2, pp. 887-897, Feb. 2019

[7] S. Yang, P. Wang and Y. Tang, "Feedback Linearization-Based Current Control Strategy for Modular Multilevel Converters," *IEEE Transactions on Power Electronics*, vol. 33, no. 1, pp. 161-174, Jan. 2018

[8] M. Ahmadijokani, M. Mehrasa, M. Sleiman, M. Sharifzadeh, A. Sheikholeslami and K. Al-Haddad, "A Back-Stepping Control Method for Modular Multilevel Converters," *IEEE Transactions on Industrial Electronics*, vol. 68, no. 1, pp. 443-453, Jan. 2021

[9] X. Zhang, J. Huang, X. Zhang and X. Tong, "Backstepping based nonlinear control strategy for MMC topology," *IECON 2017 - 43rd Annual Conference of the IEEE Industrial Electronics Society*, 2017, pp. 5707-5712

[10] M. Ishfaq et al., "Output Current Control of Modular MultiLevel Converter Using BackStepping Controller," *2019 15th International Conference on Emerging Technologies (ICET)*, 2019, pp. 1-5

[11] Z. Gong, P. Dai, X. Yuan, X. Wu and G. Guo, "Design and Experimental Evaluation of Fast Model Predictive Control for Modular Multilevel Converters," *IEEE Transactions on Industrial Electronics,* vol. 63, no. 6, pp. 3845-3856, June 2016

[12] B. Gutierrez and S. Kwak, "Modular Multilevel Converters (MMCs) Controlled by Model Predictive Control With Reduced Calculation Burden," *IEEE Transactions on Power Electronics,* vol. 33, no. 11, pp. 9176-9187, Nov. 2018

[13] M. H. Nguyen and S. Kwak, "Simplified Indirect Model Predictive Control Method for a Modular Multilevel Converter," *IEEE Access,* vol. 6, pp. 62405-62418, 2018

[14] J. Huang et al., "Priority Sorting Approach for Modular Multilevel Converter Based on Simplified Model Predictive Control," *IEEE Transactions on Industrial Electronics,* vol. 65, no. 6, pp. 4819-4830, June 2018

[15] P. Liu, Y. Wang, W. Cong and W. Lei, "Grouping-Sorting-Optimized Model Predictive Control for Modular Multilevel Converter With Reduced Computational Load," *IEEE Transactions on Power Electronics,* vol. 31, no. 3, pp. 1896-1907, March 2016

[16] M. Krstic, I. Kanellakopoulos and P. V. Kokotovic, Nonlinear and Adaptive Control Design, New York:Wiley, 1995.

[17] F. Zhang, W. Li and G. Joós, "A Voltage-Level-Based Model Predictive Control of Modular Multilevel Converter," *IEEE Transactions on Industrial Electronics*, vol. 63, no. 8, pp. 5301-5312, Aug. 2016,

[18] S. Hamayoon, M. Hovd, J. A. Suul and M. Vatani, "Modified Reduced Indirect Finite Control Set Model Predictive Control of Modular Multilevel Converters," *2020 IEEE 21st Workshop on Control and Modeling for Power Electronics (COMPEL)*, Aalborg, Denmark, 2020, pp. 1-6